Flagellin-induced NLRC4 phosphorylation primes the inflammasome for activation by NAIP5

Magdalena Matusiak[a,b], Nina Van Opdenbosch[a,b], Lieselotte Vande Walle[a,b], Jean-Claude Sirard[c], Thirumala-Devi Kanneganti[d], and Mohamed Lamkanfi[a,b,1]

[a]Department of Medical Protein Research, VIB, Ghent B-9000, Belgium; [b]Department of Biochemistry, Ghent University, Ghent B-9000, Belgium; [c]Centre d'Infection et d'Immunité de Lille, Institut Pasteur de Lille, Lille 59019, France; and [d]Department of Immunology, St. Jude Children's Research Hospital, Memphis, TN 38105-2794

Edited by Vishva M. Dixit, Genentech, San Francisco, CA, and approved December 29, 2014 (received for review September 17, 2014)

The Nlrc4 inflammasome contributes to immunity against intracellular pathogens that express flagellin and type III secretion systems, and activating mutations in NLRC4 cause autoinflammation in patients. Both Naip5 and phosphorylation of Nlrc4 at Ser533 are required for flagellin-induced inflammasome activation, but how these events converge upon inflammasome activation is not known. Here, we showed that Nlrc4 phosphorylation occurs independently of Naip5 detection of flagellin because Naip5 deletion in macrophages abolished caspase-1 activation, interleukin (IL)-1β secretion, and pyroptosis, but not Nlrc4 phosphorylation by cytosolic flagellin of *Salmonella* Typhimurium and *Yersinia enterocolitica*. ASC speck formation and caspase-1 expression also were dispensable for Nlrc4 phosphorylation. Interestingly, *Helicobacter pylori* flagellin triggered robust Nlrc4 phosphorylation, but failed to elicit caspase-1 maturation, IL-1β secretion, and pyroptosis, suggesting that it retained Nlrc4 Ser533 phosphorylating-activity despite escaping Naip5 detection. In agreement, the flagellin D0 domain was required and sufficient for Nlrc4 phosphorylation, whereas deletion of the *S.* Typhimurium flagellin carboxy-terminus prevented caspase-1 maturation only. Collectively, this work suggests a biphasic activation mechanism for the Nlrc4 inflammasome in which Ser533 phosphorylation prepares Nlrc4 for subsequent activation by the flagellin sensor Naip5.

NLRC4 | inflammasome | flagellin | caspase-1 | *Salmonella*

Inflammasomes contribute critically to immunity and antimicrobial host defense of mammalian hosts. Their activation is tightly controlled because aberrant inflammasome signaling is harmful to the host, and results in inflammatory diseases (1, 2). Inflammasomes are a set of cytosolic multiprotein complexes that recruit and activate caspase-1, a key protease that triggers secretion of the inflammatory cytokines interleukin (IL)-1β and IL-18. In addition, caspase-1 induces pyroptosis, a proinflammatory and lytic cell death mode that contributes to pathogen clearance (3, 4). Several inflammasomes respond to a distinctive set of microbial pathogens (5). Activating mutations in the nucleotide-binding and oligomerization domain (NOD)-like receptor (NLR) member Nlrc4 were recently shown to induce autoinflammation in patients (6–8). Moreover, the inflammasome assembled by Nlrc4 is critically important for clearing a variety of bacterial infections, including *Salmonella enterica* serovar Typhimurium (*S.* Typhimurium), *Shigella flexneri*, *Pseudomonas aeruginosa*, *Burkholderia thailandensis*, and *Legionella pneumophila* (3, 9–17). These intracellularly-replicating bacteria have in common that they propel themselves with flagella (18) and/or express bacterial type III secretion systems (T3SS) to translocate effector proteins into infected host cells (19). Members of the NLR apoptosis-inhibitory protein (Naip) subfamily recognize the cytosolic presence of the building blocks of these evolutionary conserved bacterial structures, and trigger Nlrc4 to assemble an inflammasome (20–25). C57BL/6J mice express four Naip proteins, Naip1, -2, -5, and -6, which are expressed from a multigene cluster located on chromosome 13qD1 (26). Mouse Naip1 and human NAIP bind T3SS needle proteins, Naip2 interacts with the T3SS basal rod component PrgJ, and Naip5 and Naip6 recognize flagellin (20, 22–25).

In addition to these Naip sensors, recent work showed that phosphorylation of Nlrc4 at Ser533 is critical for activation of the Nlrc4 inflammasome following infection with *S.* Typhimurium and *L. pneumophila*, or transfection of purified *S.* Typhimurium flagellin (27). Reconstitution of immortalized *Nlrc4*$^{-/-}$ macrophages with wild-type Nlrc4 restored *S.* Typhimurium- and *L. pneumophila*-induced inflammasome activation, whereas cells reconstituted with Nlrc4 S533A mutant were specifically defective in maturation of caspase-1, secretion of IL-1β, assembly of ASC (apoptosis-associated speck-like protein containing a CARD) specks and induction of pyroptosis by these pathogens (27). However, a central outstanding question is how these upstream events (i.e., bacterial recognition by Naip members and Nlrc4 phosphorylation) relate to each other. Naip binding of bacterial components may trigger Nlrc4 phosphorylation to induce inflammasome activation. Alternatively, Nlrc4 phosphorylation and Naip sensing of flagellin and T3SS may converge independently onto Nlrc4 inflammasome activation.

Here, we approached this question by breeding Nlrc4$^{Flag/Flag}$ mice that express Nlrc4 fused to a carboxy-terminal 3× Flag tag from both *Nlrc4* alleles (27) with Naip5-deficient mice (22, 28). We found *S.* Typhimurium infection and cytosolic delivery of *S.* Typhimurium flagellin, *S.* Typhimurium PrgJ and *Yersinia*

Significance

The Nlrc4 inflammasome is critical for clearing bacterial infections and activating mutations in NLRC4 cause autoinflammation in patients. Here, we used genetic and biochemical approaches to show that Nlrc4 Ser533 phosphorylation by flagellin of *Salmonella* Typhimurium and *Yersinia enterocolitica* occurs upstream of Naip5 detection of flagellin, ASC speck formation and caspase-1 activation. We further showed that *Helicobacter pylori* flagellin triggered robust Nlrc4 phosphorylation but failed to elicit caspase-1 activation in agreement with the differential requirement for the *Salmonella* Typhimurium flagellin D0 domain and the carboxy-terminus for Ser533 phosphorylation and caspase-1 activation, respectively. Collectively, this work suggests a biphasic mechanism for Nlrc4 inflammasome activation in which Ser533 phosphorylation primes Nlrc4 for subsequent activation by Naip5.

Author contributions: M.M. and M.L. designed research; M.M., N.V.O., and L.V.W. performed research; J.-C.S. contributed new reagents/analytic tools; M.M., N.V.O., L.V.W., T.-D.K., and M.L. analyzed data; and M.M., N.V.O., L.V.W., J.-C.S., T.-D.K., and M.L. wrote the paper.

The authors declare no conflict of interest.

This article is a PNAS Direct Submission.

Freely available online through the PNAS open access option.

[1]To whom correspondence should be addressed. Email: mohamed.lamkanfi@vib-ugent.be.

This article contains supporting information online at www.pnas.org/lookup/suppl/doi:10.1073/pnas.1417945112/-/DCSupplemental.

enterocolitica flagellin to induce Nlrc4 phosphorylation at Ser533 independently of Naip5. Interestingly, *Helicobacter pylori* (*H. pylori*) flagellin induced robust Nlrc4 Ser533 phosphorylation without caspase-1 activation, suggesting that Nlrc4 Ser533 phosphorylation and caspase-1 activation are molecularly decoupled. In agreement, the *S.* Typhimurium flagellin D0 domain was required and sufficient for Nlrc4 phosphorylation, whereas caspase-1 activation required the flagellin carboxy-terminus. Collectively, this work suggests a biphasic activation mechanism for the Nlrc4 inflammasome in which Ser533 phosphorylation primes Nlrc4 for subsequent activation by the flagellin sensor Naip5.

Results

Nlrc4 Ser533 Phosphorylation by *S.* Typhimurium Infection and SLO-Mediated Cytosolic Flagellin Occurs Upstream of Caspase-1. We made use of Nlrc4-Ser533P–specific antibodies to analyze Ser533 phosphorylation (Ser533P) in Flag-immunoprecipitates of $Nlrc4^{Flag/Flag}$ bone marrow-derived macrophages (BMDMs) that had been infected with *S.* Typhimurium. Nlrc4 phosphorylation was not readily detected in Flag-immunoprecipitates of uninfected $Nlrc4^{Flag/Flag}$ BMDMs (Fig. 1*A*). However, infection with wild-type *S.* Typhimurium triggered significant Nlrc4 phosphorylation, which coincided with maturation of procaspase-1 into its catalytic 20-kDa (p20) subunit (Fig. 1*A*). The Nlrc4 Ser533P-immunoreactive bands indeed represented phosphorylated Nlrc4 because they were not detected in setups with control agarose beads. Notably, infection with a flagellin-deficient mutant (*S.* Typhimurium Δ*fljB*Δ*fliC*) also triggered considerable Nlrc4 Ser533 phosphorylation in the absence of robust caspase-1 maturation (Fig. 1*A*), in line with the hypothesis that flagellin and the bacterial T3SS both may induce Nlrc4 phosphorylation (27). The cell-permeable caspase-1 inhibitor Ac-YVAD-cmk inhibited *S.* Typhimurium-induced caspase-1 maturation, but not Nlrc4 phosphorylation (Fig. 1*B*), confirming that the protease activity of caspase-1 was dispensable for Ser533 phosphorylation (27). To investigate whether physical recruitment of caspase-1 was needed for Nlrc4 Ser533 phosphorylation in *S.* Typhimurium-infected cells, we bred $Nlrc4^{Flag/Flag}$ mice to animals lacking expression of caspases 1 and 11 (29, 30). Expression from a single $Nlrc4^{Flag}$ allele was sufficient to monitor Nlrc4 Ser533 phosphorylation upon *S.* Typhimurium infection (Fig. S1), permitting the use of $Nlrc4^{Flag/WT}Casp1^{-/-}Casp11^{-/-}$ macrophages. Nlrc4 was robustly phosphorylated upon *S.* Typhimurium infection in both $Nlrc4^{Flag/WT}$ and $Nlrc4^{Flag/WT}Casp1^{-/-}Casp11^{-/-}$ macrophages (Fig. 1*C*), demonstrating that Nlrc4 Ser533 phosphorylation occurs upstream of caspase-1. We next used *Streptococcus pyogenes* streptolysin O (SLO) to study Nlrc4 Ser533 phosphorylation by internalized *S.* Typhimurium flagellin (fliC) in the absence of infection. LPS stimulation (Fig. S2) and SLO treatment in the absence of flagellin increased background Nlrc4 phosphorylation (Fig. 1*D*). However, cytosolic flagellin triggered robust Nlrc4 phosphorylation levels (Fig. 1*D*). Unlike cytosolic flagellin, extracellular flagellin failed to elicit Nlrc4 Ser533 phosphorylation. Moreover, only cytosolic flagellin-induced Nlrc4 phosphorylation was accompanied by caspase-1 maturation. The caspase-1 inhibitor Ac-YVAD-cmk blunted cytosolic flagellin-induced caspase-1 maturation, but not Nlrc4 Ser533 phosphorylation (Fig. 1*E*), suggesting that Nlrc4 phosphorylation was upstream of inflammasome activation. In agreement, flagellin-induced Nlrc4 phosphorylation proceeded unhampered in $Nlrc4^{Flag/WT}Casp1^{-/-}Casp11^{-/-}$ macrophages (Fig. 1*F*). Together, these results demonstrate that *S.* Typhimurium- and flagellin-induced Nlrc4 Ser533 phosphorylation occur upstream of caspase-1. In addition, they suggest that robust Nlrc4 Ser533 phosphorylation by *S.* Typhimurium Δ*fljB*Δ*fliC* is not sufficient for caspase-1 maturation.

ASC Specks Are Dispensable for *S.* Typhimurium- and Cytosolic Flagellin-Induced Nlrc4 Ser533 Phosphorylation. The adaptor protein ASC is dispensable for *S.* Typhimurium- and flagellin-induced pyroptosis, but acts upstream of caspase-1 for its maturation and IL-1β secretion (11, 31, 32). To address the role of ASC in Nlrc4 Ser533 phosphorylation, we bred $Nlrc4^{Flag/Flag}$ mice onto ASC-deficient animals (11). As shown in wild-type BMDMs (32, 33), *S.* Typhimurium infection triggered assembly of ASC specks in $Nlrc4^{Flag/WT}$ BMDMs, and this was abrogated in $Nlrc4^{Flag/WT}ASC^{-/-}$ macrophages (Fig. 2*A*). ASC specks were predominantly (80%) formed in macrophages that also contained bacteria, although they did not colocalize with intracellular EGFP-expressing *S.* Typhimurium (Fig. 2 *B* and *C*). Moreover, Nlrc4 colocalized with ASC in the specks (Fig. S3). SLO-mediated delivery of flagellin also induced ASC specks in $Nlrc4^{Flag/WT}$ BMDMs, but not in $Nlrc4^{Flag/WT}ASC^{-/-}$ macrophages (Fig. 2*A*). ASC deletion abolished *S.* Typhimurium- and SLO+flagellin-induced caspase-1 autoprocessing (Fig. 2 *D* and *E*). However, Nlrc4 Ser533 phosphorylation by *S.* Typhimurium (Fig. 2*D*) and cytosolic flagellin (Fig. 2*E*) proceeded unhampered in both $Nlrc4^{Flag/WT}$ BMDMs and $Nlrc4^{Flag/WT}ASC^{-/-}$ macrophages, demonstrating that Nlrc4 Ser533 phosphorylation occurred

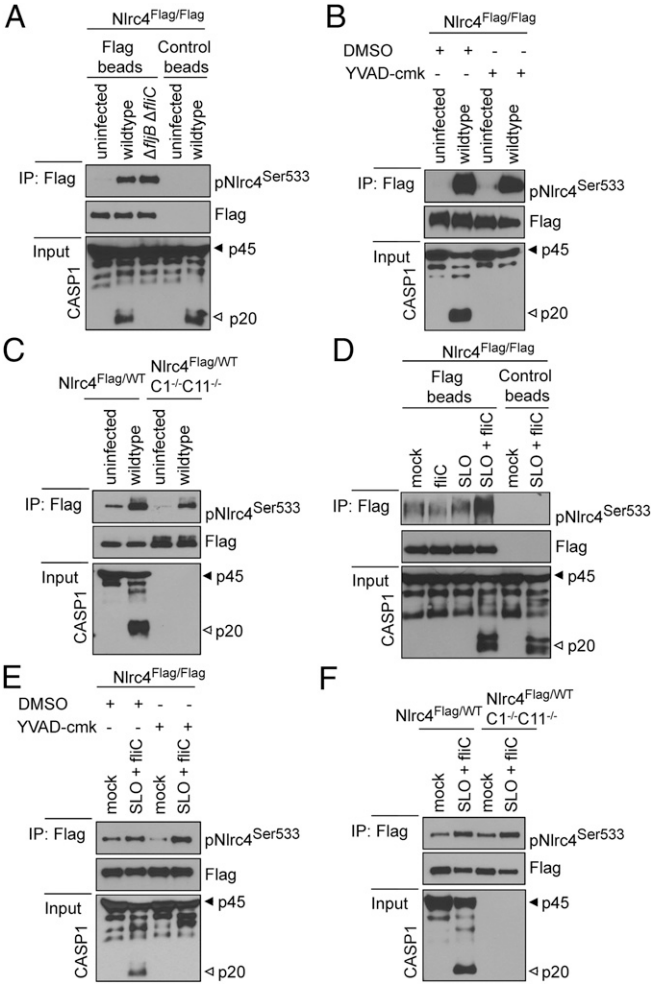

Fig. 1. NLRC4 Ser533 phosphorylation occurs upstream of caspase-1. (*A–F*) BMDMs of the indicated genotypes were infected with *S.* Typhimurium or the flagellin-deficient *S.* Typhimurium Δ*fljB* Δ*fliC* mutant (MOI 5) (*A–C*), or subjected to cytosolic delivery of fliC with streptolysin O (SLO) (*D–F*). In some setups, BMDMs were pretreated with Ac-YVAD-cmk (50 μM) for 30 min. (*B* and *E*). $Nlrc4^{Flag}$ was immunoprecipitated from cell lysates using anti-Flag beads, and NLRC4 Ser533 phosphorylation was analyzed by immunoblotting with NLRC4 phospho-Ser533–specific antibodies. Cell lysates were immunoblotted for caspase-1. Results are representative of at least three independent experiments.

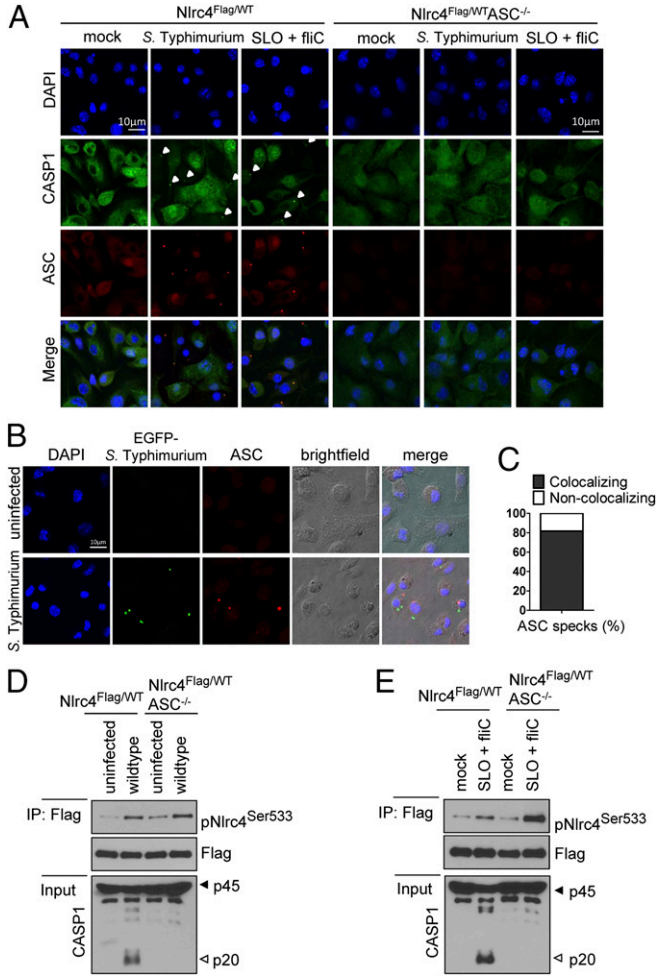

Fig. 2. ASC specks are dispensable for *S.* Typhimurium- and cytosolic flagellin-induced Nlrc4 Ser533 phosphorylation. (*A*–*C*) BMDMs were grown on coverslips and infected with *S.* Typhimurium (MOI 5) for 45 min, or treated with fliC and SLO for 20 min (*A*), or infected with EGFP-*S.* Typhimurium (MOI 5) for 45 min (*B* and *C*). Cells were immunostained for ASC (red) and caspase-1 (green). DAPI (blue) was used to localize nuclei. Arrows mark specks. Confocal micrographs were taken at 60× magnification. (*D* and *E*) BMDMs were infected with *S.* Typhimurium (MOI 5) for 60 min (*D*), or transfected with recombinant flagellin (fliC) using streptolysin O (SLO) (*E*). $Nlrc4^{Flag}$ was immunoprecipitated from cell lysates using anti-Flag beads, and NLRC4 Ser533 phosphorylation was analyzed by immunoblotting with NLRC4 phospho-Ser533–specific antibodies. Cell lysates were immunoblotted for caspase-1. Results are representative of three independent experiments.

upstream of ASC speck formation, and did not require physical interactions between Nlrc4 and ASC.

Naip5 Is Required for Flagellin-Induced Caspase-1 Activation, but Dispensable for Nlrc4 Ser533 Phosphorylation. Having established that Nlrc4 Ser533 phosphorylation occurs upstream of ASC and caspase-1, we next studied the role of Naip5. Naip5 binds flagellin and is specifically required for flagellin-induced activation of the Nlrc4 inflammasome (20, 23). As expected, *S.* Typhimurium infection-induced caspase-1 autoprocessing was severely hampered in macrophages of $Nlrc4^{Flag/Flag}$ mice that were bred onto $Naip5^{-/-}$ mice, but Nlrc4 Ser533 phosphorylation was unaffected (Fig. 3*A*). *S.* Typhimurium expresses a T3SS and flagellin, both of which may activate the Nlrc4 inflammasome. We therefore addressed the role of Naip5 upon cytosolic delivery of recombinantly purified flagellin and the T3SS rod protein PrgJ, respectively. Naip5-deficient macrophages failed to induce caspase-1 maturation (Fig. 3*B*), IL-1β secretion (Fig. 3*C*), and pyroptosis (Fig. 3*D*) upon SLO-mediated delivery of flagellin in the cytosol. However, cytosolic flagellin elicited normal Nlrc4 Ser533 phosphorylation in

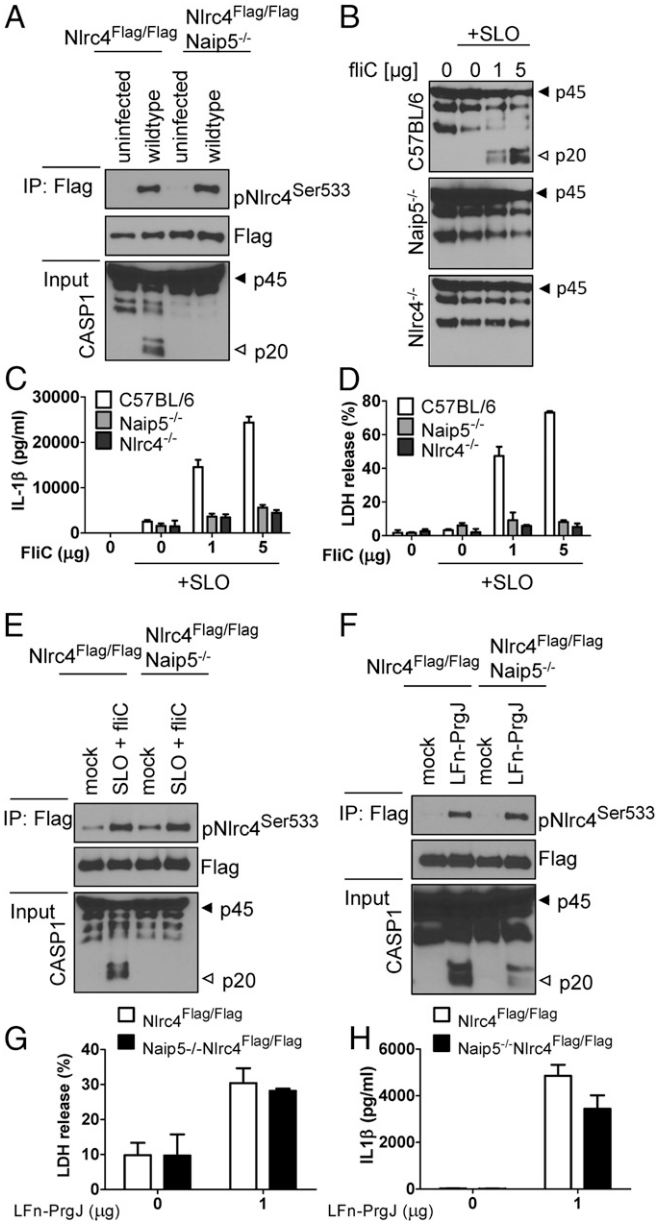

Fig. 3. Naip5 promotes flagellin-induced inflammasome activation downstream of Nlrc4 Ser533 phosphorylation. (*A*) BMDMs infected with *S.* Typhimurium (MOI 5) for 60 min. $Nlrc4^{Flag}$ was immunoprecipitated from cell lysates and subjected to immunoblotting with NLRC4 phospho-Ser533–specific antibodies. Cell lysates were immunoblotted for caspase-1. (*B*–*D*) BMDMs of the indicated genotypes were stimulated with streptolysin O (SLO) and *S.* Typhimurium flagellin (fliC). Caspase-1 autoprocessing (*B*), IL-1β secretion (*C*), and pyroptosis induction (*D*) were assessed. (*E*) BMDMs were stimulated with SLO and fliC. $Nlrc4^{Flag}$ was immunoprecipitated from cell lysates and subjected to immunoblotting with NLRC4 phospho-Ser533–specific antibodies, and cell lysates were immunoblotted for caspase-1. (*F*–*H*) BMDMs were treated with LFn-PrgJ and anthrax protective antigen (PA). $Nlrc4^{Flag}$ was immunoprecipitated from cell lysates and subjected to immunoblotting with NLRC4 phospho-Ser533–specific antibodies. Cell lysates were immunoblotted for caspase-1 (*F*). Pyroptosis induction (*G*) and IL-1β secretion (*H*) were assessed. Results are representative of at least three independent experiments.

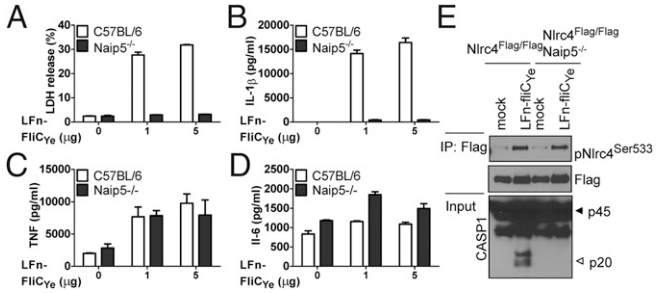

Fig. 4. *Yersinia enterocolitica* flagellin requires Naip5 for caspase-1 maturation, IL-1β secretion and pyroptosis induction, but not for Nlrc4 Ser533 phosphorylation. BMDMs were treated with *Yersinia enterocolitica* flagellin fused to the anthrax lethal factor amino-terminal-domain (LFn-fliC$_{Ye}$) and anthrax protective antigen (PA). Pyroptosis induction (*A*) and cytokine secretion (*B–D*) were assessed. (*E*) Nlrc4^{Flag} was immunoprecipitated from cell lysates and subjected to immunoblotting with NLRC4 phospho-Ser533–specific antibodies. Cell lysates were immunoblotted for caspase-1. Results are representative of at least three independent experiments.

Nlrc4$^{Flag/Flag}$Naip5$^{-/-}$ macrophages (Fig. 3*E*), demonstrating that Naip5 is dispensable for flagellin-induced Nlrc4 Ser533 activation.

PrgJ is specifically detected by Naip2 (20, 23) and anthrax protective antigen (PA)-mediated cytosolic delivery of LFn-PrgJ triggered Nlrc4 Ser533 phosphorylation in both *Nlrc4$^{Flag/Flag}$* and *Nlrc4$^{Flag/Flag}$Naip5$^{-/-}$* macrophages (Fig. 3*F*). However, *Nlrc4$^{Flag/Flag}$Naip5$^{-/-}$* macrophages consistently responded with reduced caspase-1 autoprocessing relative to *Nlrc4$^{Flag/Flag}$* macrophages (Fig. 3*F*), although the induction of pyroptosis (Fig. 3*G*) and IL-1β secretion (Fig. 3*H*) were not significantly affected. Nor was inflammasome-independent secretion of IL-6 and TNF affected (Fig. S4). Reduced caspase-1 maturation in response to intracellular LFn-PrgJ was not due to defective Naip2 expression because mRNA expression of Naip1, -2, and -6 transcripts was intact in *Naip5$^{-/-}$* macrophages (Fig. S5), which is in agreement with our recent targeted locus amplification analysis of the *Naip* multigene cluster of C57BL/6J and *Naip5$^{-/-}$* mice (28). This analysis confirmed the selective disruption of *Naip5*, and revealed the homozygous coselection of a previously undetected single nucleotide polymorphism that causes a Tyr/Asn mutation in Naip2 protein of *Naip5$^{-/-}$* mice that may mildly affect Naip2 function in these mice. Regardless, these results demonstrate that Naip5 is critical for caspase-1 activation by *S.* Typhimurium flagellin, but dispensable for Nlrc4 Ser533 phosphorylation. In addition, they imply that Naip5-mediated detection of flagellin and flagellin-induced Nlrc4 Ser533 phosphorylation are independent signals that converge upon inflammasome activation.

***Yersinia enterocolitica* Flagellin Requires Naip5 for Caspase-1 Maturation, IL-1β Secretion, and Pyroptosis Induction, but Not for Nlrc4 Ser533 Phosphorylation.** Flagellin of several bacterial pathogens elicit Nlrc4-dependent inflammasome activation (9, 10, 12, 14, 20, 22, 23), but the induction of Nlrc4 Ser533 phosphorylation has only been demonstrated for *S.* Typhimurium flagellin (27). *Y. enterocolitica* flagellin fused to the anthrax lethal factor amino-terminal domain for PA-assisted cytosolic delivery (LFn-FliC$_{Ye}$) was shown to induce Nlrc4-dependent caspase-1 maturation and pyroptosis (20). We extended these findings by demonstrating that LFn-FliC$_{Ye}$ induced pyroptosis (Fig. 4*A*), IL-1β secretion (Fig. 4*B*), and caspase-1 maturation (Fig. 4*E*) in LPS-primed wild-type macrophages, but not in Naip5-deficient cells. As a control, TNF and IL-6 secretion were not affected by Naip5 deletion (Fig. 4 *C* and *D*). However, cytosolic LFn-FliC$_{Ye}$ triggered similar levels of Nlrc4 Ser533 phosphorylation in *Nlrc4$^{Flag/Flag}$* and *Nlrc4$^{Flag/Flag}$Naip5$^{-/-}$* macrophages (Fig. 4*E*), demonstrating that *Y. enterocolitica* flagellin does not require Naip5 for Nlrc4 phosphorylation.

***Helicobacter pylori* Flagellin Induces Nlrc4 Ser533 Phosphorylation in the Absence of Caspase-1 Maturation, IL-18 Secretion, and Pyroptosis.** *H. pylori*, the primary cause of gastric ulcers and gastritis, expresses a flagellin (*H. pylori* flaA) that evades detection by the extracellular flagellin receptor TLR5 (34). However, whether *H. pylori* flagellin triggers Nlrc4 inflammasome activation is not known. *S.* Typhimurium flagellin triggered a robust and dose-dependent increase in the levels of caspase-1 maturation (Fig. 5*A*), pyroptosis (Fig. 5*B*), and IL-18 secretion (Fig. 5*C*) when delivered in the cytosol of wild-type macrophages. We also detected significant Il-1β secretion upon delivery of *S.* Typhimurium flagellin in the cytosol of LPS-primed *Nlrc4$^{Flag/Flag}$* macrophages (Fig. S6). However, none of these Nlrc4 inflammasome-dependent responses were observed with cytosolic *H. pylori* flagellin (Fig. 5 *A–C* and Fig. S6). Surprisingly, however, both *S.* Typhimurium FliC and *H. pylori* FlaA triggered robust Nlrc4 Ser533 phosphorylation (Fig. 5*D*), suggesting that *H. pylori* flagellin retained Nlrc4 Ser533-phosphorylating activity, while escaping intracellular recognition by Naip5. In addition, these results suggest that TLR5 is dispensable for flagellin-induced Nlrc4 phosphorylation.

The Flagellin D0 Domain Is Sufficient for Flagellin-Induced Nlrc4 Ser533 Phosphorylation and Inflammasome Activation. We next sought to define the flagellin requirements for Nlrc4 Ser533 phosphorylation. *S.* Typhimurium flagellin is composed of 494 amino acids that assemble into four major structural domains (Fig. 6*A*) (35, 36). Flagellin of *S.* Typhimurium and other pathogens is subject to posttranslational modifications, including *N*-methylation and glycosylation (37, 38). However, recombinant *S.* Typhimurium flagellin produced in 293T cells potently triggered caspase-1 maturation (Fig. 6*B*), suggesting that bacteria-specific posttranslational modifications of flagellin were dispensable for Naip5 detection and Naip5-independent Nlrc4 Ser533 phosphorylation. The amino- and carboxy-terminal regions (amino acids 1–43 and 454–494, respectively) are highly conserved and when recruited in the flagellum, they fold into a coiled-coil motif designated the D0 domain. We produced a number of *S.* Typhimurium flagellin mutants that were devoid of the entire D0 domain or parts thereof. Deletion of the D0 domain (fliC$_{43–450}$) abrogated the ability to induce IL-18 secretion (Fig. 6*C*), pyroptosis (Fig. 6*D*), and caspase-1 processing (Fig. 6*E*). As reported (39, 40), an *S.* Typhimurium flagellin mutant lacking only the two carboxy-terminal amino acids (fliC$_{1–492}$) also failed to activate Naip5- and Nlrc4-dependent

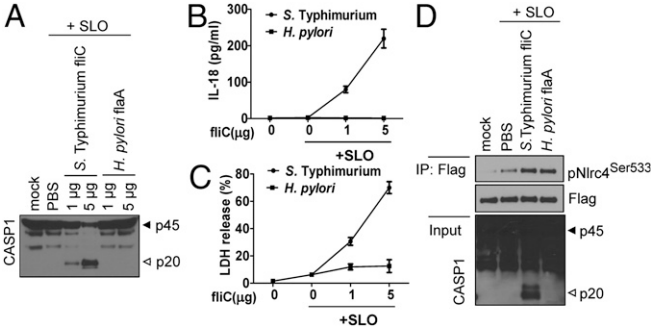

Fig. 5. *Helicobacter pylori* flagellin induces Nlrc4 Ser533 phosphorylation in the absence of caspase-1 maturation, IL-18 secretion, and pyroptosis. (*A–C*) C57BL/6J BMDMs were stimulated with *S.* Typhimurium flagellin (*S.* Typhimurium fliC) or *H. pylori* flagellin (*H. pylori* FlaA) and SLO. Caspase-1 autoprocessing (*A*), IL-18 secretion (*B*), and pyroptosis induction (*C*) were assessed. (*D*) *Nlrc4$^{Flag/Flag}$* BMDMs were stimulated with streptolysin O (SLO) and *S.* Typhimurium flagellin (*S.* Typhimurium fliC) or *H. pylori* flagellin (*H. pylori* FlaA). Nlrc4^{Flag} was immunoprecipitated from cell lysates and subjected to immunoblotting with NLRC4 phospho-Ser533–specific antibodies. Cell lysates were immunoblotted for caspase-1. Results are representative of at least three independent experiments.

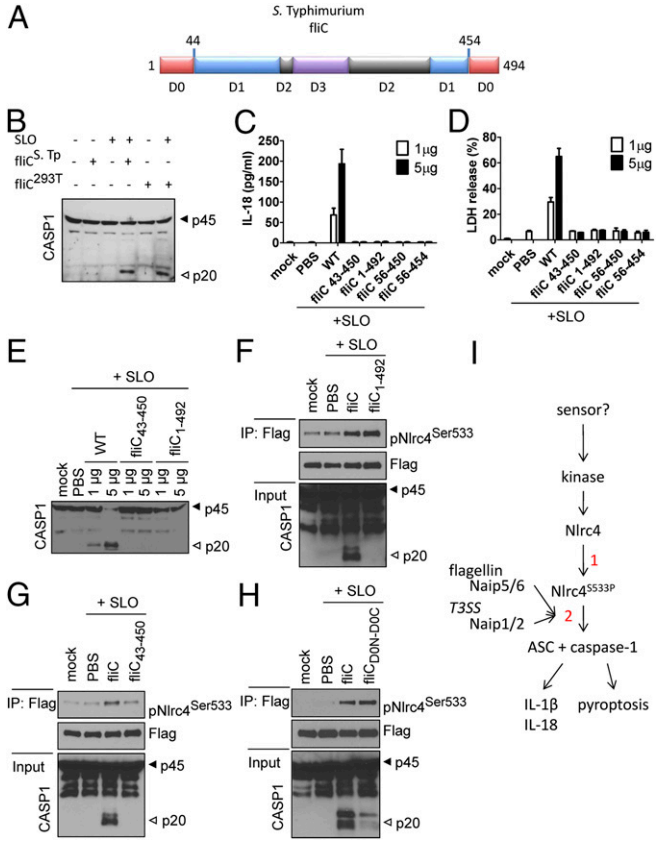

Fig. 6. The flagellin D0 domain mediates Nlrc4 Ser533 phosphorylation. (*A*) Schematic representation of *S.* Typhimurium fliC domain structure. Regions are color-coded according to the corresponding structural domains (D0, D1, D2, and D3). (*B*) C57BL/6J BMDMs were left untreated or transfected with recombinant fliC that was purified from bacteria or produced in 293T cells. Caspase-1 processing was assessed by immunoblotting. (*C–E*) C57BL/6J BMDMs were stimulated with SLO and indicated mutants of *S.* Typhimurium flagellin. IL-18 secretion (*C*), pyroptosis induction (*D*), and caspase-1 autoprocessing (*E*) were assessed. (*F–H*) *Nlrc4*$^{Flag/Flag}$ BMDMs were simulated with *S.* Typhimurium flagellin (fliC) or indicated fliC mutants and SLO. Nlrc4^{Flag} was immunoprecipitated from cell lysates and subjected to immunoblotting with NLRC4 phospho-Ser533–specific antibodies. Cell lysates were immunoblotted for caspase-1. Results are representative of three independent experiments. (*I*) Schematic model of biphasic Nlrc4 inflammasome activation depicting priming of Nlrc4 by Ser533 phosphorylation (step 1), and Nlrc4 activation by Naip recognition of bacterial factors (Step 2).

inflammasome responses (Fig. 6 *C–E*). However, fliC$_{1–492}$ was fully capable of inducing Nlrc4 Ser533 phosphorylation upon its cytosolic delivery (Fig. 6*F*), demonstrating that, although critical for Nlrc4 inflammasome activation, the flagellin carboxy-terminus was dispensable for Nlrc4 phosphorylation. In contrast, Nlrc4 phosphorylation by the fliC$_{43–450}$ mutant lacking the amino- and carboxy-terminal D0 motifs was markedly diminished (Fig. 6*G*), suggesting that Nlrc4 Ser533 phosphorylation was mediated by the FliC D0 domain. In agreement, cytosolic delivery of a flagellin mutant composed solely of the amino- and carboxy-terminal D0 motifs (fliC$_{D0N-D0C}$) triggered Nlrc4 Ser533 phosphorylation to levels that were comparable to those induced by full-length fliC (Fig. 6*H*). Notably, fliC$_{D0N-D0C}$ also induced caspase-1 autoprocessing, although with reduced efficiency compared with full-length fliC (Fig. 6*H*). These results suggest that the D0 domain is sufficient for both Nlrc4 Ser533 phosphorylation and Naip5-dependent inflammasome activation, but additional fliC domains may enhance Naip5 detection of flagellin.

Discussion

Together with the demonstrated roles of both Naip proteins and Nlrc4 Ser533 phosphorylation for inflammasome activation by *S.* Typhimurium and cytosolic flagellin (20, 23, 27), the findings presented here support a biphasic activation model of the Nlrc4 inflammasome (Fig. 6*I*). In this model, detection of cytosolic flagellin and/or the T3SS rod component PrgJ induces Nlrc4 Ser533 phosphorylation, which primes, but is not sufficient to activate Nlrc4 (Step 1). Nlrc4 inflammasome assembly requires subsequent interaction of Naip5 with the flagellin carboxy-terminus or detection of the T3SS by Naip1/2 (Step 2), which may recruit phosphorylated Nlrc4 to the complex and induce conformational changes in the latter that result in inflammasome assembly and caspase-1 activation. Such two-step regulation of Nlrc4 inflammasome activation may prevent the inadvertent induction of deleterious inflammatory responses, and ensure that initiation of pyroptosis induction and secretion of IL-1β and IL-18 occurs only in infected macrophages. A biphasic activation mechanism is not unique for the Nlrc4 inflammasome. The Nlrp3 inflammasome is generally considered to be controlled by separate priming and activation steps (5). Moreover, the proposed model clarifies the "closed conformation" of the recently reported crystal structure of phosphorylated Nlrc4 (21). In agreement with the results presented here, Nlrc4 Ser533 phosphorylation did not result in an "open" conformation that is believed to be required for recruitment of caspase-1 (21). However, interactions of the Ser533 phosphate group with the carboxy-terminal HD2 and LRR regions may promote Nlrc4 inflammasome assembly under physiological conditions by facilitating the disengagement of the carboxy-terminus from the amino-terminal region of Nlrc4.

In conclusion, we showed here that Nlrc4 Ser533 phosphorylation by flagellin of *S.* Typhimurium, *Y. enterocolitica*, and *H. pylori* occurs independently of Naip5. Moreover, Nlrc4 Ser533 phosphorylation required the *S.* Typhimurium flagellin D0, whereas deletion of the flagellin carboxy-terminus was sufficient to halt Naip5-dependent caspase-1 activation. Unlike with *S.* Typhimurium and *Y. enterocolitica* flagellin, *H. pylori*-induced Nlrc4 Ser533 phosphorylation was not accompanied by Nlrc4 inflammasome activation. The identification of distinct structural requirements for Naip5-independent Nlrc4 Ser533 phosphorylation and Naip5-mediated inflammasome activation revealed sequential priming and activation steps for activation of the Nlrc4 inflammasome.

Experimental Procedures

Mice. *Nlrc4*$^{Flag/Flag}$ (27), *Nlrc4*$^{-/-}$ (11), and *ASC*$^{-/-}$ (11) mice have been described, and were kindly provided by V. M. Dixit (Genentech, San Francisco). *Naip5*$^{-/-}$ (22) and *Casp1*$^{-/-}$*11*$^{-/-}$ (30) mice obtained from R. Vance (University of California, Berkeley, CA) and R. Flavell (Yale University, New Haven, CT), respectively. Mice were housed in individually ventilated cages and kept under pathogen-free conditions at animal facilities of Ghent University. All animal experiments were conducted with permission of the Ethical committees on laboratory animal welfare of Ghent University.

Cell Preparation, Reagents, and Stimulation. Bone marrow-derived macrophages (BMDMs) were generated as described (31). Cells were seeded in 12-well plates (1×10^6 cells per well) and infected with *S.* Typhimurium or flagellin-deficient *S.* Typhimurium (ΔfljBΔfliC) at multiplicity of infection (MOI 5) for 60 min. Gentamycin (50 μg/mL, 10131–027, Life Technologies) was added, and cell lysates were prepared 30 min later. In other experiments, recombinant *H. pylori* flagellin (flaA, HPA-5040, Austral Biologicals), or purified *S.* Typhimurium flagellin (fliC, 5 μg/mL) produced in *E. coli* (40) or 293T cells (fliC^{293T}) was delivered in the cytosol using streptolysin O (SLO, 25 μg/mL, S5265-25KU, Sigma), as described (17). In some experiments, cells were pretreated with Ac-YVAD-cmk (50 μM, ALX-260–028-M001, Enzo Life Sciences) for 30 min before *S.* Typhimurium infection or fliC transfection. Otherwise, cells were treated with anthrax protective antigen (1 μg/mL, List Biologicals) and 1 μg/mL LFn-PrgJ (20).

Bacteria. EGFP-*S.* Typhimurium was made by electroporating bacteria cultured in the presence of L(+) arabinose (1.33 mM, A3256, Sigma) with EGFP-pBAD (54762, Addgene).

Immunoprecipitation. Cell lysates were collected together with culture media in cell lysis buffer (20 mM Tris·HCl pH 7.4, 200 mM NaCl, 1% Nonidet P-40) supplemented with Complete Protease Inhibitor Mixture tablets (05892970001, Roche). Lysates were immunoprecipitated using anti-Flag agarose (A2220-1ML, Sigma) and eluted with 3× Flag peptide according to the manufacturer's instructions (F4799-4MG, Sigma).

Western Blotting. Protein samples were denatured in Laemmli buffer, incubated at 95 °C for 10 min and separated by SDS/PAGE. Separated proteins were transferred to PVDF membranes. Immunoblots were incubated with primary antibodies against Flag (1/5,000, A8592-2MG, Sigma), caspase-1 (1/1,000, AG-20B-0042-C10, Adipogen), and Nlrc4^{Ser533P} (Gen-82 clone 3–3, ½,000, Genentech; and a custom-made affinity-purified Nlrc4^{Ser533P}-specific polyclonal antibody raised against peptide *N*-LWRQEp**S**IQSLR-C; Pacific Immunology). Proteins were detected by enhanced chemiluminescence.

Cytokine Analysis and LDH Measurement. Cytokines were measured by Luminex assay (Bio-Rad) and IL1β ELISA (R&D Systems), according to the manufacturers' instructions. Cell death was determined by LDH assay (G1780, Promega).

ASC Speck Analysis by Confocal Microscopy. Macrophages plated in chamber slides were left untreated or infected with *S.* Typhimurium (MOI 5) or EGFP-*S.* Typhimurium (MOI 5) for 45 min. Alternatively, cells were transfected with recombinant fliC (5 μg/mL) using SLO. Cells were fixed with 4% paraformaldehyde, permeabilized using 0.1% Triton-X100, and stained with antibodies against ASC (1/400, AG-25B-0006, Adipogen) and caspase-1 (1/200, AG-20B-0042-C100, Adipogen). Secondary antibodies were anti–rabbit Alexa Fluor 594 and anti-mouse Alexa Fluor 488 (1/250, A-11029 and A-11037, Life Technologies). Slides were mounted with ProLong Gold Antifade reagent with DAPI (P36935, Life Technologies). Confocal micrographs were taken on an Olympus FV10-ASW (version 2.0) laser scanning microscope and FV10-ASW4.1 software.

RT-PCR. Total RNA was isolated using RNeasy kit (74104, Qiagen). cDNA was synthesized using the QuantiTect Reverse Transcription kit (205311, Qiagen). Quantitative PCR (qPCR) was performed on triplicate samples using LightCycler 480 SYBR Green I Master Mix kit (4707516001, Roche) in a LightCycler 480 real-time PCR machine (Roche). The cycling conditions were 95 °C for 5 min followed by 45 cycles of 95 °C for 10 s, 60 °C for 15 s, and 72 °C for 20 s. Gene expression levels were normalized to β-actin and GAPDH. Primers used for RT-PCR were: GAPDH, 5′-GGTGAAGGTCGGTGTGAACG3′ and 5′CTCGCTCCTGGAAGATGGTG3′; β-actin, 5′GTCGACAACGGCTCCGGC3′ and 5′GGTGTGGTGCCAGATTTTCT3′; Naip1, 5′GCTTACTGCAACGACAGCGTCTTCG3′ and 5′CTGGAATCACTTCTGCAGAGGACTTCG3′; Naip2, 5′TGTAGCTTGATCCTCTTTTCCAC3′ and 5′TGCACAGTGTCCCTTTTACCTG3′; Naip5, 5′CACACGTGAAAGCAACCATGG3′ and 5′GTTGAGATTGGAGAAGACCTCG3′; Naip6, 5′AGGATGTTTGGAGAAGTGGGC3′ and 5′GGCAAGTTCATGTGGCAGAAAC3′.

Statistics. GraphPad Prism 5.0 software was used for data analysis. Data are shown as mean with SD. Data were compared by an unpaired two-tailed Student's *t* test. $P < 0.05$ was considered to indicate statistical significance.

ACKNOWLEDGMENTS. We thank Dr. Vishva M. Dixit (Genentech), Dr. Richard Flavell (Yale University), and Dr. Russell Vance (University of California, Berkeley) for generous supply of mutant mice. We also thank Dr. Vishva M. Dixit for supply of Nlrc4^{Ser533P} antibody and Dr. Feng Shao (National Institute of Biological Sciences) for *Y. enterocolitica* LFn-FlaA and *S.* Typhimurium LFn–PrgJ fusion proteins. L.V.W. is supported by a postdoctoral fellowship from the Fund for Scientific Research-Flanders. T.-D.K. is supported by National Institute of Health Grants AR056296, CA163507, and AI101935 and grants from the American Lebanese Syrian Associated Charities (ALSAC). This work was supported by Ghent University Grants BOF 01N02313 and 01J11113, Fund for Scientific Research-Flanders Grant G030212N, and European Research Council Grant 281600 (to M.L.).

1. Lamkanfi M, Dixit VM (2012) Inflammasomes and their roles in health and disease. *Annu Rev Cell Dev Biol* 28:137–161.
2. Strowig T, Henao-Mejia J, Elinav E, Flavell R (2012) Inflammasomes in health and disease. *Nature* 481(7381):278–286.
3. Miao EA, et al. (2010) Caspase-1-induced pyroptosis is an innate immune effector mechanism against intracellular bacteria. *Nat Immunol* 11(12):1136–1142.
4. Bergsbaken T, Fink SL, Cookson BT (2009) Pyroptosis: Host cell death and inflammation. *Nat Rev Microbiol* 7(2):99–109.
5. Lamkanfi M, Dixit VM (2014) Mechanisms and functions of inflammasomes. *Cell* 157(5):1013–1022.
6. Canna SW, et al. (2014) An activating NLRC4 inflammasome mutation causes autoinflammation with recurrent macrophage activation syndrome. *Nat Genet* 46(10):1140–1146.
7. Kitamura A, Sasaki Y, Abe T, Kano H, Yasutomo K (2014) An inherited mutation in NLRC4 causes autoinflammation in human and mice. *J Exp Med* 211(12):2385–2396.
8. Romberg N, et al. (2014) Mutation of NLRC4 causes a syndrome of enterocolitis and autoinflammation. *Nat Genet* 46(10):1135–1139.
9. Amer A, et al. (2006) Regulation of Legionella phagosome maturation and infection through flagellin and host Ipaf. *J Biol Chem* 281(46):35217–35223.
10. Franchi L, et al. (2006) Cytosolic flagellin requires Ipaf for activation of caspase-1 and interleukin 1beta in salmonella-infected macrophages. *Nat Immunol* 7(6):576–582.
11. Mariathasan S, et al. (2004) Differential activation of the inflammasome by caspase-1 adaptors ASC and Ipaf. *Nature* 430(6996):213–218.
12. Miao EA, et al. (2006) Cytoplasmic flagellin activates caspase-1 and secretion of interleukin 1beta via Ipaf. *Nat Immunol* 7(6):569–575.
13. Suzuki T, et al. (2007) Differential regulation of caspase-1 activation, pyroptosis, and autophagy via Ipaf and ASC in Shigella-infected macrophages. *PLoS Pathog* 3(8):e111.
14. Sutterwala FS, et al. (2007) Immune recognition of Pseudomonas aeruginosa mediated by the IPAF/NLRC4 inflammasome. *J Exp Med* 204(13):3235–3245.
15. Miao EA, Ernst RK, Dors M, Mao DP, Aderem A (2008) Pseudomonas aeruginosa activates caspase 1 through Ipaf. *Proc Natl Acad Sci USA* 105(7):2562–2567.
16. Franchi L, et al. (2007) Critical role for Ipaf in Pseudomonas aeruginosa-induced caspase-1 activation. *Eur J Immunol* 37(11):3030–3039.
17. Lamkanfi M, et al. (2007) The Nod-like receptor family member Naip5/Birc1e restricts Legionella pneumophila growth independently of caspase-1 activation. *J Immunol* 178(12):8022–8027.
18. Macnab RM (2003) How bacteria assemble flagella. *Annu Rev Microbiol* 57:77–100.
19. Cornelis GR (2006) The type III secretion injectisome. *Nat Rev Microbiol* 4(11):811–825.
20. Zhao Y, et al. (2011) The NLRC4 inflammasome receptors for bacterial flagellin and type III secretion apparatus. *Nature* 477(7366):596–600.
21. Hu Z, et al. (2013) Crystal structure of NLRC4 reveals its autoinhibition mechanism. *Science* 341(6142):172–175.
22. Lightfield KL, et al. (2008) Critical function for Naip5 in inflammasome activation by a conserved carboxy-terminal domain of flagellin. *Nat Immunol* 9(10):1171–1178.
23. Kofoed EM, Vance RE (2011) Innate immune recognition of bacterial ligands by NAIPs determines inflammasome specificity. *Nature* 477(7366):592–595.
24. Rayamajhi M, Zak DE, Chavarria-Smith J, Vance RE, Miao EA (2013) Cutting edge: Mouse NAIP1 detects the type III secretion system needle protein. *J Immunol* 191(8):3986–3989.
25. Yang J, Zhao Y, Shi J, Shao F (2013) Human NAIP and mouse NAIP1 recognize bacterial type III secretion needle protein for inflammasome activation. *Proc Natl Acad Sci USA* 110(35):14408–14413.
26. Wright EK, et al. (2003) Naip5 affects host susceptibility to the intracellular pathogen Legionella pneumophila. *Curr Biol* 13(1):27–36.
27. Qu Y, et al. (2012) Phosphorylation of NLRC4 is critical for inflammasome activation. *Nature* 490(7421):539–542.
28. de Vree PJ, et al. (2014) Targeted sequencing by proximity ligation for comprehensive variant detection and local haplotyping. *Nat Biotechnol* 32(10):1019–1025.
29. Kayagaki N, et al. (2011) Non-canonical inflammasome activation targets caspase-11. *Nature* 479(7371):117–121.
30. Kuida K, et al. (1995) Altered cytokine export and apoptosis in mice deficient in interleukin-1 beta converting enzyme. *Science* 267(5206):2000–2003.
31. Van Opdenbosch N, et al. (2014) Activation of the NLRP1b inflammasome independently of ASC-mediated caspase-1 autoproteolysis and speck formation. *Nat Commun* 5:3209.
32. Broz P, von Moltke J, Jones JW, Vance RE, Monack DM (2010) Differential requirement for Caspase-1 autoproteolysis in pathogen-induced cell death and cytokine processing. *Cell Host Microbe* 8(6):471–483.
33. Broz P, et al. (2010) Redundant roles for inflammasome receptors NLRP3 and NLRC4 in host defense against Salmonella. *J Exp Med* 207(8):1745–1755.
34. Andersen-Nissen E, et al. (2005) Evasion of Toll-like receptor 5 by flagellated bacteria. *Proc Natl Acad Sci USA* 102(26):9247–9252.
35. Samatey FA, et al. (2001) Structure of the bacterial flagellar protofilament and implications for a switch for supercoiling. *Nature* 410(6826):331–337.
36. Yonekura K, Maki-Yonekura S, Namba K (2003) Complete atomic model of the bacterial flagellar filament by electron cryomicroscopy. *Nature* 424(6949):643–650.
37. Logan SM (2006) Flagellar glycosylation - a new component of the motility repertoire? *Microbiology* 152(Pt 5):1249–1262.
38. Smith KD, et al. (2003) Toll-like receptor 5 recognizes a conserved site on flagellin required for protofilament formation and bacterial motility. *Nat Immunol* 4(12):1247–1253.
39. Miao EA, et al. (2010) Innate immune detection of the type III secretion apparatus through the NLRC4 inflammasome. *Proc Natl Acad Sci USA* 107(7):3076–3080.
40. Van Maele L, et al. (2014) Airway structural cells regulate TLR5-mediated mucosal adjuvant activity. *Mucosal Immunol* 7(3):489–500.